Journal of Pharmaceutical and Biomedical Analysis 51 (2010) 1–6

Contents lists available at ScienceDirect

Journal of Pharmaceutical and Biomedical Analysis

journal homepage: www.elsevier.com/locate/jpba

On-chip assay for determining the inhibitory effects and modes of action of drugs against xanthine oxidase

Pravin K. Naoghare [a], Ho Taik Kwon [b], Joon Myong Song [a,*]

[a] Research Institute of Pharmaceutical Sciences, College of Pharmacy, Seoul National University, 599, Gwanangno, Gwanak gu, Seoul 151-742, South Korea
[b] 8F-8, Hightech Center, Gyeonggi Technopark, Celltek Co., Ltd., Ansan-si 426-170, South Korea

ARTICLE INFO

Article history:
Received 30 April 2009
Received in revised form 15 July 2009
Accepted 16 July 2009
Available online 24 July 2009

Keywords:
Xanthine oxidase
Nitroblue tetrazolium
Photodiode array
High-throughput screening
Drug discovery screening

ABSTRACT

Xanthine oxidase (XO) is a key enzyme that can catalyze the conversion of xanthine to uric acid, causing various diseases in humans. We have developed a high-throughput chip-based assay that uses a photodiode array (PDA) microchip system to explore the inhibitory effects of drug analogs on XO. Inhibitory activities of cyclosporin A, aminoglutethimide, dithranol and naringenin against XO were assessed using this chip-based xanthine assay in the presence or absence of the antioxidant enzyme, superoxide dismutase (SOD). In addition, the mechanism of drug action was also disclosed by monitoring the combined effect of respective drug analogs and SOD on XO in the assay. The assessment was based on the red light absorption property of nitroblue tetrazolium (NBT) formazan, formed by free radical-mediated NBT reduction. Compared to naringenin (50 and 100 μM; a known XO inhibitor), cyclosporin A (5 and 10 μM) exhibited similar XO inhibitory activity, whereas dithranol (1 and 3 μM) and aminoglutethimide (2.5 and 5 mM) showed minimum XO inhibition. Low standard deviation obtained during the assay demonstrates the preciseness and accuracy of the developed approach. Compared to the existing methods, the developed approach is advantageous due to its simplicity and compatibility with high-throughput screening procedures. Furthermore, this approach can be applied to the early phase of drug discovery screening to explore various drug analogs for their XO inhibitory activities.

1. Introduction

Xanthine oxidase (XO), a form of xanthine oxidoreductase, catalyzes the last two steps of purine catabolism, *i.e.*, the oxidation of hypoxanthine to xanthine and xanthine to uric acid [1]. XO plays an important role in various ischemic tissues [2], vascular injuries [3], inflammatory diseases [3], and chronic heart failure [4]. It is also a major source of free radicals (superoxide) that can vitiate energy metabolism and decrease energetic efficiency [4]. XO activity contributes significantly to the degree of oxidative stress, brain edema, thermal stress, respiratory syndrome, viral infection, and hemorrhagic shock *in vivo* [5–7]. It is also associated with gout (metabolic arthritis), a crystal deposition disease attributed to the elevated levels of uric acid (hyperuricemia) in the bloodstream [8]. Thus, XO inhibition has been proposed as a mechanism for curing cardiovascular health, oxidative stress, inflammatory diseases and vascular injuries [9,10]. In the recent past, several drug analogs (allopurinol, oxypurinol, phytic acid, tisopurine, etc.) that inhibit xanthine oxidase were proposed for the treatment of hyperuricemia and gout [11]. Allopurinol has been the prototypic XO inhibitor over the last few decades [12]. Apart from its beneficial effects, serious toxicities appear in patients and lead to renal failure, *i.e.*, allopurinol hypersensitivity syndrome. Other XO inhibitors like oxypurinol, phytic acid and tisopurine also impart toxic effects in the patients in a dose-dependent manner [13,14]. While a significant part of modern pharmaceutical research is focused on exploring new drug analogs as potent XO inhibitors with more therapeutic efficacy and less toxicity, considerable time and money are also being spent to develop new high-throughput methodologies to evaluate the efficacy of the potent drug candidates.

Different technologies allowing insight into genomic and postgenomic modifications have been developed as tools for detecting and understanding the drug-driven XO inhibition. Microarray has been used to assess the inhibitory effects of drugs on the transcriptome profiles of the XO gene [15]. Success has been limited with this approach as the mechanistic targets for XO inhibition are not always confined by the transcriptome profiling alone due to their post-transcriptional modifications [16]. Methods for elucidating the alterations in the translational profiles of XO protein after a designated drug treatment have also been proposed. However, these methods involve either cumbersome manual or expensive robotic operations to obtain high-density cell cultures in multi-well format [17]. Recently, microfabricated miniaturized devices have been recognized as potential platforms for screening XO inhibitors.

* Corresponding author. Tel.: +82 2 880 7841; fax: +82 2 871 2238.
E-mail address: jmsong@snu.ac.kr (J.M. Song).

0731-7085/$ – see front matter © 2009 Elsevier B.V. All rights reserved.
doi:10.1016/j.jpba.2009.07.020

These devices, consisting of micro-channels/micro-detectors, have facilitated high-throughput detection of analytes using microliter or nanoliter volumes of test samples [18]. Chip assays based on surface plasmon resonance (SPR) [19], forster resonance energy transfer (FRET) [20] and immunolabeling have been applied to elucidate the drug-induced XO inhibition. However, these assays are tedious as they require probing of target DNA/antigens onto the chip sensing surface and/or labeling with expensive fluorescent indicators (organic dyes, quantum dots, etc.) to elucidate the drug-driven XO inhibition [19,20]. In addition, other impeding factors such as poor resolution of refractive index (RI) of analytes (in SPR), cross talk between donor and acceptor dyes (in FRET), photobleaching of commercially used fluorophores, low detection limit of devices and the complexity in data interpretation limit the overall utility of these techniques. Hence, new screening methodologies are needed to explore XO inhibitors in a simple, low-cost and high-throughput manner.

Here, we describe the development of a photodiode array (PDA) chip-based xanthine assay for high-throughput screening of XO inhibitors using a PDA microchip system [21,22]. Inhibitory effects of dithranol (anthracene derivative), aminoglutethimide (anti-steroid), cyclosporin A (immunosuppressant) and naringenin (flavonoid) on XO were elucidated using the chip-based assay in the presence or absence of a free radical scavenging enzyme (SOD, superoxide dismutase). Drug analogs were assessed for their ability to inhibit XO, which leads to a reduction in the conversion of nitroblue tetrazolium (NBT) to NBT diformazan. The developed chip-based assay is compatible for high-throughput drug screening as the assay requires microliter amounts of reaction samples that can be directly spotted onto a chip consisting of an array (12×12) of photodiode elements. It does not require probing of target biomolecules on the chip surface or fluorophore labeling procedures and thus eliminates undesired cross talk between the fluorophores. Consistent results can be achieved as the measurements based on the light absorption properties of NBT formazan provide background-subtracted absolute values in the presence of drugs analogs compared to their respective controls.

In this work, the colorimetric bioassay has unique properties for high-throughput drug screening compatible with the PDA microchip platform. The colorimetric reaction based on the conversion of NBT to NBT formazan allows multivariate drug screening applications wherein the XO inhibitory and toxic activities of drug analogs can be simultaneously monitored using the chip-based xanthine assay. Detection of absorption by the final reaction product and photosensitivity of the constructed PDA microchip system facilitate quantitative assessment of drug activity. In addition, the on-chip colorimetric bioassay does not require the series of complicated and careful surface treatments for the immobilization of XO target protein that is required for conventional high-throughput protein-based drug screening such as surface plasmon resonance.

2. Experimental

2.1. Materials

Superoxide dismutase (SOD), xanthine, xanthine oxidase, dithranol, aminoglutethimide, cyclosporin A, naringenin, nitroblue tetrazolium (NBT), phosphate-buffered saline (PBS; 10 mM, pH 7), ethanol, acetone and other materials were obtained from Sigma (St. Louis, MO). All chemicals and reagents are of the highest purity available and used without further purification.

2.2. On-chip xanthine assay

All assay procedures were carried out at room temperature. Stock solutions of SOD (1 U/μl), dithranol (100 μM), aminoglutethimide (100 mM), cyclosporin A (100 μM) and naringenin (1 mg/ml) were prepared in PBS, acetone, PBS, ethanol and dimethyl sulfoxide (DMSO), respectively. All stock solutions were made fresh on the day of use. Xanthine oxidase solution (0.125 U/mL) was prepared in PBS (10 mM, pH 7) containing 100 μM diethylenetriaminepentaacetic acid (DTPA) and kept in an ice bath. Xanthine solution (100 mM) was prepared in PBS (10 mM, pH 7) containing 0.05N sodium hydroxide. Reaction medium contained PBS (10 mM, pH 7), 3 mM xanthine, 0.025 U/mL xanthine oxidase, 3.8×10^{-6} mol/L NBT and the test sample [dithranol (1 and 3 μM), aminoglutethimide (2.5 and 5 mM), cyclosporin A (5 and 10 μM), naringenin (50 and 100 μM) and/or SOD enzyme (1–10 U)] in a total assay volume of 100 μL. A control reaction was carried out wherein all the assay conditions and reagents were identical to those above, except that the test sample (drugs and/or SOD enzyme) was substituted with an equal volume of PBS. Reaction tubes were centrifuged (13,000 rpm/5 min), supernatant was decanted and the insoluble formazan was dissolved in formaldehyde solution (Sigma; 37% by weight in water). Reaction samples (5 μL) were directly spotted on the PDA chip. Our earlier publication explains the construction of the PDA chip and the microchip system in detail [21,22]. Briefly, the PDA microchip system comprised a test board and an array of light-emitting diodes (LEDs). The PDA chip employed in this study was constructed using conventional bipolar semiconductor technology. It is composed of p–n junction and another n-type impurity (n+) doped into the n-type silicon to induce a higher leakage current. Photodiode generates the photocurrent which flows into the current amplifier by a piece of aluminum (the first metal). To protect the current amplifier from exposure to ambient light another piece of aluminum (the second metal) was used. Each photodiode dimensions were 300 μm × 300 μm and the distance between photodiode-to-photodiode was 100 μm. Each photodiode of the chip is covered with silicon nitride (Si_3N_4) to minimize the damage of photodiode from the direct exposure of test sample. The PDA chip was composed of 12×12 detection elements and was mounted in the center of the test board. In this configuration, a uniform and intense red beam of light produced by the LEDs hits the photodiode elements of the PDA chip and generates photosignals. Each signal from the photodiode detection elements is individually addressed by a digital input/output (I/O) line and the analog-to-digital converter supplied by an RS232 interface. The PDA chip was placed at the center of the test board and the photosignals were measured. Custom software programmed in C language was used to operate the data acquisition process.

2.3. Native gel electrophoresis

Alterations in the SOD (0.1 U) activities in reaction mixtures containing the appropriate drugs were measured by native gel (10%) electrophoresis. As described by Beauchamp and Fridovich [23], gel was rinsed with deionized water (18.2 MΩ) and incubated in NBT (2.5 mmol/L) for 30 min in the dark. The gel was rinsed with deionized water and then incubated in riboflavin (1.17×10^{-6} mol/L) for 20 min in the dark. The gel was again washed with deionized water and exposed to light (light intensity of 25–1000 μEinstein/m^2/s) using a fiber optic light source (Nikon, Japan). Through a photochemical reaction, NBT was reduced to blue-colored NBT formazan except at positions where SOD was localized.

3. Results and discussion

The present work entails the development of a chip-based xanthine assay to explore the XO inhibitory properties of drug analogs. Fig. 1 illustrates the schematics of our approach. The reduction of NBT to NBT formazan in the presence of XO and drug analog can be

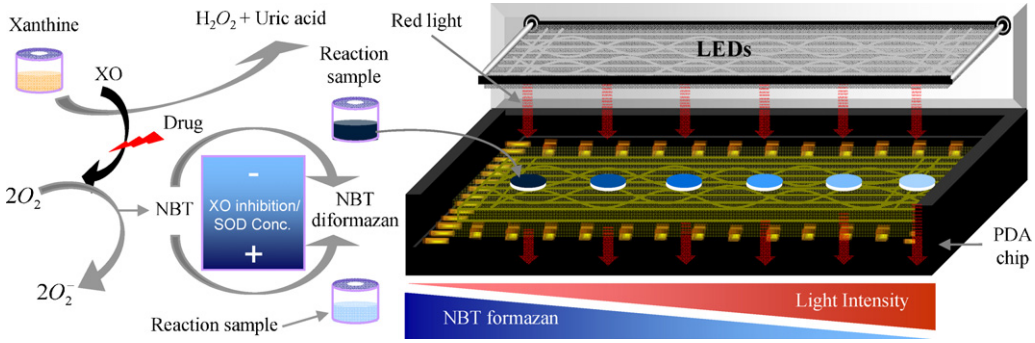

Fig. 1. Schematic of the chip-based xanthine assay, demonstrating the induction of free radicals (O_2^-) due to the oxidation of xanthine by XO and the conversion of NBT to NBT diformazan. The reduction in the development of NBT formazan was directly proportional to the SOD concentration and the extent of XO inhibition by the respective drug analog. Reaction samples were directly spotted on the photodiode elements of the PDA chip. The reduction in the red light intensity was indirectly proportional to the reduction in the development of NBT diformazan.

seen. The PDA microchip system employed in this study consists of an array of red light-emitting diodes (LEDs) focused precisely onto the photodetectors of the PDA chip (Fig. 1). Thus, the photosignals generated by the PDA chip are directly related to the intensity of red light (emitted by LEDs) reaching the photodiodes. Blue-colored NBT formazan present in the reaction sample absorbs the red light and thereby lowers the photosignal. The red light absorption property of NBT formazan was employed for on-chip XO inhibitory activity measurements. The drug analog in the chemical reaction inhibits XO thereby lowering the production of free radicals (O_2^-) and the carryover product (O_2 and H_2O_2). This in turn inhibits the development of NBT formazan in the reaction. Thus, comparison of the inhibition of NBT formazan production in reaction samples to that in their controls is a means for estimating the XO inhibitory activity of the respective drug analog.

To establish the relative estimation of NBT formazan production in the assay, the photoresponse of the PDA chip (Fig. 2A) was measured against varying concentrations of SOD. Output voltages from six different photodiode elements spotted with reaction sample were gathered and averaged. Relative reduction in output voltage (ΔS) was calculated from the averages of output voltages obtained from three different chips. ΔS signifies the ratio of the variations in

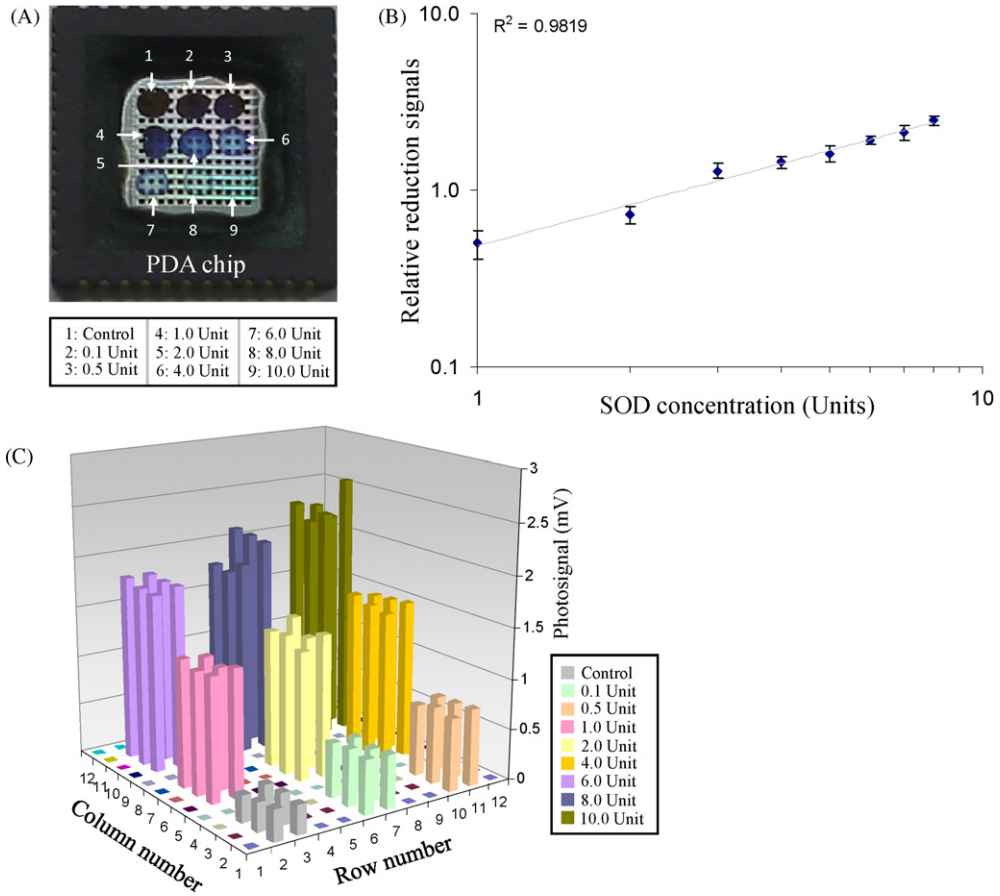

Fig. 2. On-chip estimation of SOD activity. (A) Photo image of PDA chip spotted with the reaction samples. Free radicals produced during the assay convert NBT to NBT diformazan. After the assay, reaction samples were directly spotted on the PDA chip. (B) Dependence of relative inhibition signals on the SOD concentration in the reaction sample. Output voltages were gathered from six detection photodiodes on three individual chips. Relative reduction in photosignal (ΔS; *Y*-axis) was plotted against reaction sample (*X*-axis) containing increasing amounts of SOD (1–10 U). (C) 3D graph illustrating the consistent output signals obtained from the PDA chip.

average output signal of control and sample to the average output signal of the control. Under a given set of conditions, the reduction of the photosignal was directly related to the concentration of NBT formazan present in the reaction sample. The photodiode elements spotted with the reaction samples were screened from the irradiated red light. As shown in Fig. 2B, the *X*-axis represents SOD concentration (0.1–10 U) and the *Y*-axis (ΔS) represents the inhibition signals, *i.e.*, the reduction in the light intensity reaching the photodiode element in the presence of the test samples (with SOD) compared to their respective controls (without SOD). The relative inhibition signals were linear at SOD concentrations ranging from 0.1 to 10 U (linear regression coefficient, $R^2 = 0.98$). Thus, higher ΔS values signify higher SOD activities in the reaction samples. For each sample, the standard deviation of the ΔS values obtained from three different measurements was less than 5%. The standard error of estimation was as low as 0.026. The linear dependence of ΔS values with the amount of SOD illustrates that SOD in the assay reaction inhibited NBT formazan development in a linear fashion. Therefore the relative inhibition signal for the control sample was lower than that of the tested samples. The same can be observed in the 3D graph (Fig. 2C) wherein the consistency in output signals obtained from the chip-based assay can be seen. Here, the *X* and *Y* axes represent the row and column numbers of the 12×12 photodiode array microchip, and the *Z*-axis represents the photosignals (mV) obtained after the on-chip assay. The low standard deviation achieved during the assay may be attributed to the presence of homogeneous NBT formazan over the photodiodes and the consistent photoresponse of the constructed PDA chip.

To demonstrate the accuracy of the developed assay, results were further compared with the grayscale intensities of the same reaction samples (spotted onto the PDA chip) as described in Fig. 2A. Fig. 3A depicts a line graph wherein the variation in the grayscale values of reaction samples can be seen. Here, the *X*-axis represents the increasing concentration of SOD enzyme with respect to the sample number (1–9) and the *Y*-axis represents the grayscale intensities obtained by commercially available software (MetaMorph, Version 7.1.3.0, Molecular Devices). Grayscale values were taken randomly from six different regions of an individual reaction sample spotted onto the PDA chip. To achieve this, edge detection convolution was applied to a micrograph of the PDA chip spotted with reaction samples (Fig. 3A, inset). The result showed that differences in the grayscale values of reaction samples were not sufficient to demonstrate linearity (linear regression coefficient, $R^2 = 0.65$) in grayscale values with increasing concentrations of SOD enzyme in the assay reaction. The 3D graph (Fig. 3B) clearly depicts the inconsistency in output signals obtained from grayscale measurements. Higher standard deviation obtained during the measurements signified that the estimations based on the grayscale intensities were inappropriate for the relative quantitative analysis of NBT formazan.

To explore the efficacy of the developed assay, drug analogs were screened for their XO inhibitory activities and compared with a known XO inhibitor, naringenin [24]. In the last few decades, the XO inhibitory activities of many drug analogs have been investigated. Indeed, the specific inhibitory activity of allopurinol against XO has increased its popularity since 1964 [12]. Since then, many chemical analogs (phytic acid, myo-inositol, oxypurinol, febuxostat, etc.) have been screened for their XO inhibitory activities. However, the adverse side effects of these compounds have reduced their clinical applications. Pacher and co-workers reported the toxic effects of oxypurinol on human subjects. The untoward effects of such compounds have led to a search for alternative drugs with non-toxic and specific XO inhibitory effects [25]. Thus, in the present study, we screened the drug analogs to explore their XO inhibitory activities. Fig. 4 shows the screening of four drug analogs in the chip-based xanthine assay. The ability of drugs to inhibit XO was assessed based on NBT reduction. Free radicals produced due to the oxidation of

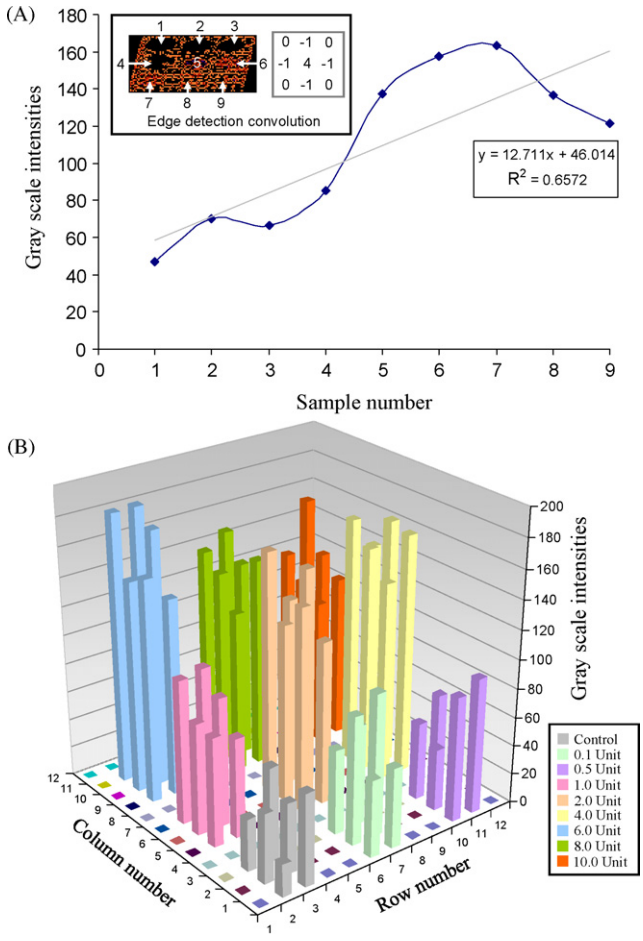

Fig. 3. (A) Line graph depicting the variation in the grayscale intensities of reaction samples spotted onto the PDA chip. Inset shows the micrograph of the PDA chip spotted with the reaction samples after edge detection convolution. Here, numerals on the *X*-axis and on the PDA chip micrograph (inset), *i.e.*, 1, 2, 3, 4, 5, 6, 7, 8 and 9, represent control, 0.1 U, 0.5 U, 1.0 U, 2.0 U, 4.0 U, 6.0 U, 8.0 U and 10.0 U of SOD enzyme, respectively. (B) 3D graph illustrating the inconsistencies in output signals based on the grayscale intensities. Here, the *X* and *Y* axes represent the array (12×12) of row and column of the photodiode array microchip whereas the *Z*-axis represents the variations in the grayscale intensities.

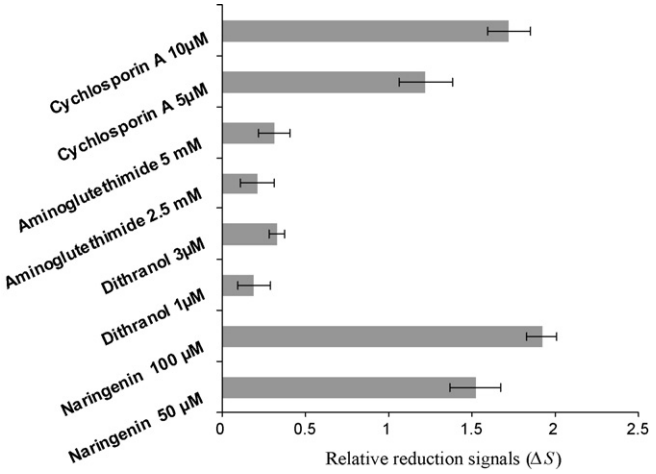

Fig. 4. Effect of drug analogs on XO activity. Increases in the ΔS values correspond to increases in XO inhibitory activity. XO inhibitory activity of cyclosporin A, aminoglutethimide and dithranol was compared to that of a known XO inhibitor, naringenin. Error bars on the *Y*-axis refer to the deviations in the ΔS values obtained from three individual experiments.

Table 1
Relative inhibition signals (ΔS) obtained through chip-based SOD assay. Higher ΔS values indicate higher XO inhibitory and SOD activity in the respective test sample.

Sr. no.	Test samples	ΔS values
1	Naringenin	
	50 μM	1.52
	100 μM	1.92
2	Dithranol	
	1 μM	0.19
	3 μM	0.33
3	Aminoglutethimide	
	2.5 mM	0.21
	5 mM	0.31
4	Cyclosporin A	
	5 μM	1.22
	10 μM	1.72
5	Naringenin + SOD (0.1 U)	
	50 μM	2.06
	100 μM	2.26
6	Dithranol + SOD (0.1 U)	
	1 μM	0.31
	3 μM	0.41
7	Aminoglutethimide + SOD (0.1 U)	
	2.5 mM	0.38
	5 mM	0.45
8	Cychlosporin A + SOD (0.1 U)	
	5 μM	1.16
	10 μM	1.53

xanthine by XO resulted in the reduction of NBT to insoluble NBT formazan.

In order to achieve homogeneous distribution of NBT formazan over the photodiode elements, insoluble NBT formazan was dissolved in formaldehyde solution (Sigma; 37% by weight in water) and the reaction samples were directly spotted on the photodiode elements of the PDA chip (Fig. 3A). ΔS values for each individual reaction sample were obtained as described above. In Fig. 4, the *X*-axis represents the drug analogs used in the xanthine assay and the *Y*-axis represents the relative reduction signals (ΔS) obtained from the PDA chip. The results indicate that the ΔS values differed for each sample.

Compared to naringenin (50 and 100 μM), aminoglutethimide (2.5 and 5 mM) and dithranol (1 and 3 μM) showed lower XO inhibitory activities (lower ΔS values). Cyclosporin A (5 and 10 μM) exhibited similar XO inhibitory activities compared to naringenin (Table 1). The mechanism by which naringenin inhibits XO involves its surface activity. As a flavonoid, naringenin has a greater number of aromatic hydroxyl groups. The concomitant hydrophilicity and hydrophobicity within the naringenin molecule helps it to bind the active motifs of XO enzyme more strongly, thereby reducing the XO activity. However, the inhibition of XO by naringenin is moderate due to the presence of glycosyl groups [26]. Iio et al. reported that the bulky and hydrophilic nature of the glycosyl groups prohibits glycosidic flavonoids from coming into contact with the XO enzyme [27]. Madesh and Balasubramanian reported that cyclosporin A inhibits xanthine and xanthine oxidase complexes in mitochondrial phospholipase D-activated rat enterocytes [28]. However, the mechanism by which cyclosporin A inhibits XO is not well understood. The chip-based xanthine assay showed higher XO inhibitory activities of cyclosporin A, which were similar to those of naringenin, hence supporting the data reported by Madesh and Balasubramanian. Compared to naringenin and cyclosporin A, aminoglutethimide and dithranol did not significantly inhibit XO. To date, there are no available reports illustrating the inhibitory effect of aminoglutethimide and dithranol on XO,

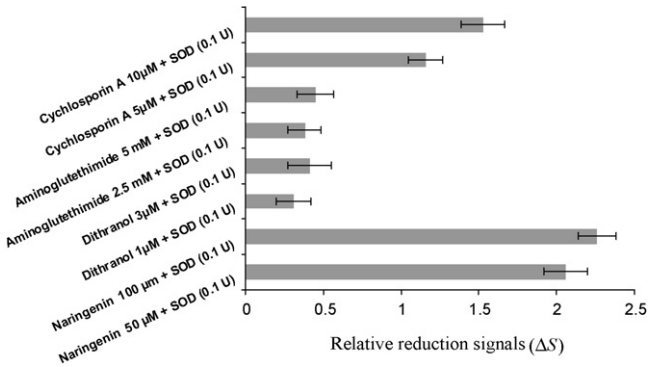

Fig. 5. High-throughput XO inhibitory and SOD activity assessment through chip-based assay. XO inhibitory activities of drug analogs were tested in the presence of a radical scavenging enzyme, SOD. Variations in the ΔS values refer to the alterations in XO inhibitory and SOD activity.

which supports our results. XO has been reported as a potential source of oxygen-derived free radicals during the reperfusion of ischemic myocardium and in other disease states. Recent reports suggest that XO inhibitors (allopurinol and oxypurinol) relieve the ischemic-reperfused myocardium by salvaging free radicals, and not by inhibiting XO in the pig heart [29]. Therefore, for better insight into the mode of action of the respective drug analogs, we investigated the effect of drugs on XO in the presence and absence of a radical scavenging enzyme (SOD). Fig. 5 illustrates a high-throughput drug screening assay in the presence of XO enzyme and a radical scavenging enzyme, SOD. Here, the *X*-axis corresponds to the drug analogs and SOD (0.1 U) and the *Y*-axis represents ΔS values obtained from the on-chip assay. As seen in Fig. 5, aminoglutethimide (2.5 and 5 mM) and dithranol (1 and 3 μM) showed minimum increase in the relative reduction signals in the presence of SOD, whereas a moderate increase in ΔS values was observed when the assay was carried out in the presence of cyclosporin A (5 and 10 μM) and 0.1 U of SOD enzyme (Table 1). A marked increase in the relative reduction signal was recorded when naringenin (50 and 100 μM) and SOD enzyme (0.1 U) were used in the assay. The obtained results were used to correlate the mode of action of the tested drug analogs with XO inhibition.

All the tested drug analogs, except naringenin, are reported to produce free radicals both *in vivo* and *in vitro* [25,29]. Cyclosporin A causes hypoxia and increases the production of free radicals, leading to renal injury through hypoxia-reoxygenation [30]. Krauskopf et al. reported that the cyclosporin A-generated free radicals are independent of cytochrome P-450 (CYP) metabolism [31]. Similarly, aminoglutethimide is reported to induce free radicals by metabolizing myeloperoxidase [32]. In the case of dithranol, the free radical production is related to its rapid auto-oxidation [33]. *In vivo* studies have demonstrated that dithranol generates reactive oxygen intermediates (ROI) during its inflammatory response against various cellular moieties. Thus, the moderate (in the case of cyclosporin A) and the minimum (in the case of aminoglutethimide and dithranol) effects of drugs in the presence of SOD may be attributed to their ROI-generating abilities [30,31]. Drug-induced radicals generated during the assay consumed most of the SOD enzyme, thereby lowering the ΔS values. In contrast, a marked increase in ΔS values in the presence of naringenin and SOD may be attributed to their antioxidant properties. Naringenin is a flavonoid that is considered to have a bioactive effect on human health as an antioxidant, a free radical scavenger, an anti-inflammatory, a carbohydrate metabolism promoter, and an immune system modulator [34]. Naringenin exerts nephrotoxic and antioxidant effects in various *in vivo* and *in vitro* models [24]. Thus, it can be concluded that the combined antioxidant effect of naringenin and SOD enzyme, along with naringenin

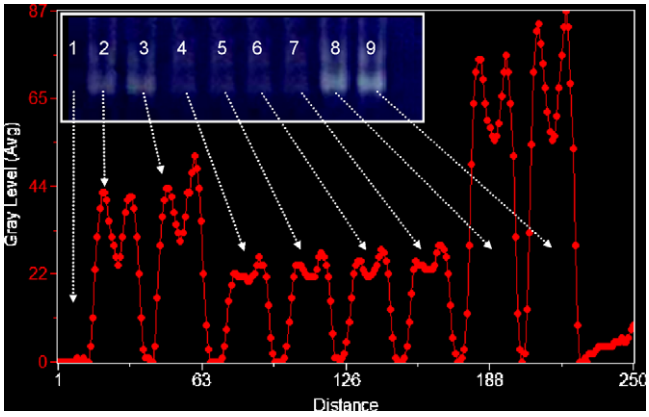

Fig. 6. Average grayscale intensities of SOD enzymes were obtained by MetaMorph software after native gel electrophoresis and activity staining of SOD enzyme. *X*-axis of the line graph represents distance whereas *Y*-axis represents average grayscale values. Here, (1) Control, (2) cyclosporin A 5 μM + SOD (0.1 U), (3) cyclosporin A 10 μM + SOD (0.1 U), (4) aminoglutethimide 2.5 mM + SOD (0.1 U), (5) aminoglutethimide 5 mM + SOD (0.1 U), (6) dithranol 1 μM + SOD (0.1 U), (7) dithranol 3 μM + SOD (0.1 U), (8) naringenin 50 μM + SOD (0.1 U), and (9) naringenin 100 μM + SOD (0.1 U).

XO inhibitory effects, inhibited the XO-driven radical production in the assay reaction, resulting in higher ΔS values.

Fig. 6 depicts the average grayscale intensities of the SOD enzymes after native gel electrophoresis. The inset shows the gel image after native staining for SOD enzyme. The obtained results clearly demonstrate that the SOD activities in the presence of naringenin were higher compared to those with aminoglutethimide and dithranol; moderate SOD activities were observed in the presence of cyclosporin A. Thus, it can be inferred that the interaction of respective drug analogs with SOD altered the SOD activities. These results are consistent with the results obtained via the chip-based assay (Fig. 5) and hence validate our approach. By using marketed drugs (cyclosporin A, aminoglutethimide, dithranol and naringenin) as examples, we have shown the application of the on-chip xanthine assay for high-throughput screening of XO inhibitors. In addition, the mode of action of the respective drug analogs was also revealed by implementing a known antioxidant enzyme (SOD) in the assay reaction.

4. Conclusion

Inhibition of XO is a key for improving various disease states in humans. The scarcity and toxicity of existing XO inhibitors demand new methodologies in order to explore new candidates as potent and non-toxic sources for XO inhibition. Herein, we report a new high-throughput chip-based xanthine assay to explore the XO inhibitory properties of drug analogs, along with their modes of action. The work presented here has important implications with regard to rapid and automated drug discovery screening processes in the pharmaceutical industry. The developed chip-based assay can be used as an efficient alternative to various MEMS and other miniaturized systems for high-throughput drug discovery screening.

Acknowledgments

This work was supported by Nuclear Research & Program of the Korea Science and Engineering Foundation (KOSEF) grant funded by the Korean government (MEST) (grant code 2009-0062225) and Korea Institute of Environmental Science and Technology (KIEST) as “The Eco-technopia 21 project”. (101-091-040).

References

[1] H.M. Martin, J.T. Hancock, V.R. Harrison, Infect. Immun. 72 (2004) 4933–4939.
[2] T. Yasuda, T. Yoshida, A.E. Goda, M. Horinaka, K. Yano, T. Shiraishi, M. Wakada, Y. Mizutani, T. Miki, T. Sakai, Mol. Cancer Res. 6 (2008) 1852–1860.
[3] J. Wu, J.G. Hecker, N. Chiamvimonvat, Adv. Drug Deliv. Rev. 61 (2009) 351–363.
[4] A. Dhoble, V. Balakrishnan, R. Smith, Cases J. 1 (2008) 238.
[5] P. Christopher, K.G. Kathy, Trends Cardiovasc. Med. 17 (2007) 48–54.
[6] S. Basuroy, S. Bhattacharya, C.W. Leffler, H. Parfenova, Am. J. Physiol. Cell Physiol. 296 (2009) 422–432.
[7] J. Reyes, W.P. Leary, Cardiovasc. Drugs Ther. 19 (2005) 311–313.
[8] E.E. Kelley, A. Trostchansky, H. Rubbo, B.A. Freeman, R. Radi, M.M. Tarpey, J. Biol. Chem. 279 (2004) 37231–37234.
[9] S. Muraoka, T. Miura, Life Sci. 74 (2004) 1691–1700.
[10] V.R. Winrow, J.D. Perry, Ann. Rheum. Dis. 46 (1987) 493–494.
[11] F. Arellano, J.A. Sacristan, Ann. Pharmacother. 27 (1993) 337–343.
[12] V. Lissandron, A. Terrin, M. Collini, L. D'alfonso, G. Chirico, S. Pantano, M. Zaccolo, J. Mol. Biol. 354 (2005) 546–555.
[13] A.V. Naumova, V.P. Chacko, R. Ouwerkerk, L. Stull, E. Marbán, R.G. Weiss, Am. J. Physiol. Heart Circ. Physiol. 290 (2006) 837–843.
[14] J. George, A.D. Struthers, Cardiovasc. Ther. 26 (2008) 59–64.
[15] N. Linder, C. Haglund, M. Lundin, S. Nordling, A. Ristimäki, A. Kokkola, J. Mrena, J.-P. Wiksten, J. Lundin, J. Clin. Pathol. 59 (2006) 965–971.
[16] I. Lenaerts, B.P. Braeckman, F. Matthijssens, J.R. Vanfleteren, Anal. Biochem. 311 (2002) 90–92.
[17] N. Linder, J. Lundin, J. Isola, M. Lundin, K.O. Raivio, H. Joensuu, Clin. Cancer Res. 11 (2005) 4372–4381.
[18] K.Y. Yan, R.L. Smith, S.D. Collins, Biomed. Microdevices 2 (2000) 1572–8781.
[19] W. Tonomura, H. Okamura, S. Konishi, IEEJ Trans. Electr. Electron. Eng. 2 (2007) 372–377.
[20] R. Dronov, D.G. Kurth, H. Mohwald, F.W. Scheller, F. Lisdat, Electrochim. Acta 53 (2007) 1107–1113.
[21] J.M. Song, M.-S. Yang, H.T. Kwan, Biosens. Bioelectron. 22 (2007) 1447–1453.
[22] P.K. Naoghare, H.T. Kwon, J.M. Song, Lab Chip 7 (2007) 1202–1205.
[23] A. Beauchamp, I. Fridovich, Anal. Biochem. 44 (1971) 276–287.
[24] H. Kogler, H. Fraser, S. McCune, R. Altschuld, E. Marbán, Cardiovasc. Res. 59 (2003) 582–592.
[25] P. Pacher, A. Nivorozhkin, C. Szabo, Pharmacol. Rev. 58 (2006) 87–114.
[26] J. Viguier, L. d'Alteroche, L. Picon, D. Karsenti, M. Guerin, Y. Bacq, E.H. Metman, Gastroenterol. Clin. Biol. 21 (1997) 342.
[27] M. Iio, A. Moriyama, Y. Matsumoto, N. Takaki, M. Fukumoto, Agric. Biol. Chem. 49 (1985) 2173–2176.
[28] M. Madesh, K.A. Balasubramanian, Biochim. Biophys. Acta (BBA)—Lipids Lipid Metab. 1389 (1998) 206–212.
[29] T.P. Dew, A.J. Day, M.R.A. Morgan, J. Agric. Food Chem. 53 (2005) 6510–6515.
[30] S.P. Bruce, Ann. Pharmacother. 40 (2006) 2187–2194.
[31] A. Krauskopf, T.M. Buetler, N.S.D. Nguyen, K. Macé, U.T. Ruegg, Br. J. Pharmacol. 135 (2002) 977–986.
[32] H. Takahama, T. Minamino, H. Asanuma, M. Fujita, T. Asai, M. Wakeno, H. Sasaki, H. Kikuchi, K. Hashimoto, N. Oku, M. Asakura, J. Kim, S. Takashima, K. Komamura, M. Sugimachi, N. Mochizuki, M. Kitakaze, J. Am. Coll. Cardiol. 53 (2009) 709–717.
[33] Z. Zhong, X. Li, S. Yamashina, M.v. Frankenberg, N. Enomoto, K. Ikejima, M. Kolinsky, J.A. Raleigh, R.G. Thurman, J. Pharmacol. Exp. Ther. 299 (2001) 858–865.
[34] A.G. Siraki, M.G. Bonini, J. Jiang, M. Ehrenshaft, R.P. Mason, Chem. Res. Toxicol. 20 (2007) 1038–1045.